

# Wind-Tunnel Study of a Circulation-Controlled Elliptical Airfoil

T. A. Stevenson,\* M. E. Franke,† and W. E. Rhynard Jr.‡

*Air Force Institute of Technology*

and

J. R. Snyder§

*Wright-Patterson Air Force Base, Ohio*

A circulation control method for increasing the low-speed lift characteristics of an elliptically shaped airfoil is investigated in wind-tunnel tests. Circulation control is achieved from a jet of air that exits through a 0.02-in. spanwise slot along the upper surface of the airfoil near the trailing edge. The lift is shown to increase with increase in blowing rates. The added lift is attained at small or even negative angles of attack with relatively small amounts of blowing air. A splitter plate attached to the lower surface of the airfoil is shown to increase the lift and improve the lift-to-drag ratio. The splitter plate, however, causes the drag to increase at low rates of blowing, but reduces the drag under some conditions at higher blowing rates.

## Nomenclature

- $b$  = splitter plate chord  
 $c$  = airfoil chord  
 $C_d$  = section total drag coefficient  
 $C_{dr}$  = section profile drag coefficient (wake rake)  
 $C_l$  = section lift coefficient,  $C_n \cos \alpha$   
 $C_n$  = section normal force coefficient,

$$\int_0^l (C_{pl} - C_{pu}) d(x/c)$$

- $C_p$  = pressure coefficient,  $(p - p_0)/q_0$   
 $C_\mu$  = momentum coefficient,  $\dot{m}V_j/(q_0 c)$   
 $D$  = section drag  
 $h$  = wind-tunnel test section height  
 $L$  = section lift  
 $L/D$  = section lift-to-drag ratio,  $C_l/C_d$   
 $\dot{m}$  = jet mass flow rate per unit span  
 $p$  = static pressure  
 $q$  = dynamic pressure,  $\rho V^2/2$   
 $Re$  = Reynolds number,  $\rho V_0 c/\mu$   
 $V$  = velocity  
 $x$  = chordwise coordinate  
 $y$  = coordinate normal to chord  
 $\alpha$  = geometric angle of attack  
 $\alpha_{eff}$  = effective angle of attack,  $\alpha - \alpha_i$   
 $\alpha_i$  = induced angle of attack  
 $\beta$  = splitter plate deflection from airfoil chord  
 $\mu$  = viscosity  
 $\rho$  = density

## Subscripts

- $j$  = slot  
 $l$  = lift or lower surface  
 $0$  = freestream  
 $u$  = upper surface

## Introduction

THERE is considerable interest in devices that improve the low-speed, high-lift capability of aircraft. This interest has developed in attempting to meet requirements for shorter distances for takeoff and landing, reduced landing velocities, increased endurance, and direct lift control. Particular applications include fixed-wing STOL aircraft and possible use on helicopter rotors.<sup>1-9</sup> To meet the requirements of high lift at low speed, various methods have been used, such as boundary-layer control by blowing and suction, circulation control by blowing, jet flaps, externally blown flaps, various combinations and variations of the above as well as other arrangements of slots, slats, and flaps. One of the main differences between these high-lift devices and conventional lifting devices is that the high-lift devices are generally powered to some degree. This means the wing lift is augmented by engine power in some manner and requires integrating the lifting and propulsion systems.

The object of the investigation described herein is to study a circulation control method using blowing for increasing the low-speed lift characteristics of an elliptical airfoil. Relatively high-speed air is blown over the rear upper surface of the airfoil and attaches to the blunt trailing edge by the Coanda effect. This changes the airfoil front and rear stagnation points and increases the circulation about the airfoil. The result is an increase in lift. This method of increasing the lift is relatively simple and has the advantage of generating large lift forces at small or even negative angles of attack while using only small amounts of blowing air.

In addition to the power required to maintain the flow of blowing air, there is also relatively high drag associated with the mixing of the blowing air and the freestream and the separation of the blowing air near the trailing edge of the airfoil.<sup>1-4</sup> Kind and Maull<sup>1</sup> found that a small splitter plate attached to the lower surface of the trailing edge reduced the mixing losses and improved the lift-to-drag ratio, but their results were somewhat preliminary. Consequently, this study further considers the use of a splitter plate and its effect on lift and drag.

Wind-tunnel tests are conducted to determine the effectiveness of the circulation-controlled airfoil and the effects of the blowing rate and the splitter plate on lift and drag at various angles of attack. The results are presented in terms of the pressure coefficient, section lift coefficient, section drag coefficient, and lift-to-drag ratio. Some potential flow solutions using Theodorsen's transformation are given to compare with the experimental pressure distributions.

Presented as Paper 76-933 at the AIAA Aircraft Systems and Technology Meeting, Dallas, Texas, Sept. 27-29, 1976; received Sept. 29, 1976; revision received April 19, 1977.

Index categories: Aerodynamics; Performance; Jets, Wakes, and Viscid-Inviscid Flow Interactions.

\*Captain, USAF; presently Foreign Technology Division, Wright-Patterson Air Force Base, Ohio. Member AIAA.

†Professor. Member AIAA.

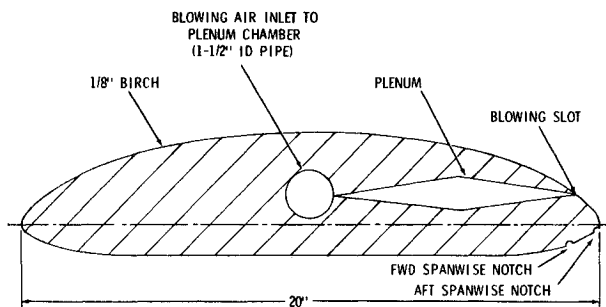
‡Captain, USAF; presently Air Force Armament Laboratory, Eglin AFB, Fla. Member AIAA.

§Senior Design Engineer, Aeronautical Systems Division.

**Table 1** Location of static pressure taps on the upper and lower surfaces of the airfoil

Upper surface pressure tap	$x/c$	$y/c$	Lower surface pressure tap	$x/c$	$y/c$
0 (LE)	0	0	22 (TE)	1.000	0
1	0.0066	0.0243	1	0.0066	-0.0081
2	0.0182	0.0401	2	0.0182	-0.0134
3	0.0355	0.0551	3	0.0355	-0.0185
4	0.0582	0.0702	4	0.0582	-0.0234
5	0.0716	0.0773	5	0.0716	-0.0258
6	0.0862	0.0841	6	0.0862	-0.0280
7	0.1020	0.0908	7	0.1020	-0.0302
8	0.1562	0.1089	8	0.1562	-0.0363
9	0.1975	0.1194	9	0.1975	-0.0398
10	0.2422	0.1285	10	0.2422	-0.0428
11	0.2900	0.1361	11	0.2900	-0.0454
12	0.3925	0.1465	12	0.3925	-0.0488
13	0.5000	0.1500	13	0.5000	-0.0500
14	0.6074	0.1465	14	0.6574	-0.0475
15	0.7099	0.1361	15	0.7099	-0.0454
16	0.8026	0.1194	16	0.8026	-0.0398
17	0.8439	0.1089	17	0.8439	-0.0363
18	0.8981	0.0908	18	0.9418	-0.0234
19	0.9284	0.0773	19	0.9645	-0.0185
20	0.9818	0.0401	20	0.9818	-0.0134
21	0.9934	0.0243	21	0.9934	-0.0081
19Lt <sup>a</sup>	0.9284	0.0773			
19Rt <sup>a</sup>	0.9284	0.0773			
20Lt <sup>a</sup>	0.9818	0.0401			
20Rt <sup>a</sup>	0.9818	0.0401			

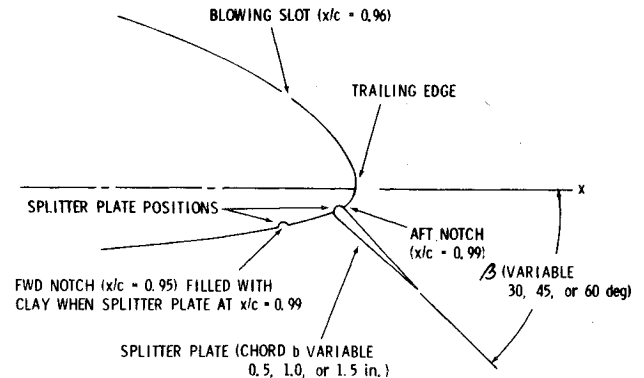
<sup>a</sup> The pressure tap is located 6 in. to the left (Lt) or right (Rt) of the airfoil center span.

**Fig. 1** Sketch of airfoil without splitter plate (clean).

### Description of the Airfoil

The airfoil used in this study was a 20% thick elliptical airfoil with a 5% camber. This airfoil is similar to the uncambered airfoil used by Kind and Maull,<sup>1</sup> but differs because of the 5% camber. A schematic of the airfoil is shown in Fig. 1. The airfoil had a chord of 1.67 ft and a span of 2.17 ft. The blowing slot consisted of a uniform 0.02-in. opening along the span at 96% chord. The blowing air entered the airfoil through a 1.5-in.-i.d. pipe and passed through a converging-diverging plenum before exiting through the 0.02-in. slot. The slot exit was directed approximately parallel to the chord and, consequently, made an angle of approximately 35 deg with the airfoil surface. Forty-eight pressure taps were used to measure the static pressure along the upper and lower surfaces of the airfoil at the locations given in Table 1. Forty-four of these taps were located at the center span and four taps were located off the center span to check the uniformity of the flow.

In order to reduce the mixing losses on the airfoil, a splitter plate was located on the lower surface of the airfoil near the blunt trailing edge. The effects of splitter plate chord, location, and angle of lift and drag were studied during the tests. A schematic of the trailing-edge section with the splitter plate at 99% chord is shown in Fig. 2. Tests were run with the

**Fig. 2** Sketch of trailing edge with 1.5-in. chord splitter plate at  $x/c = 0.99$ .

splitter plate at two different airfoil chord positions (95% and 99% chord), with three different chords (0.5, 1.0, and 1.5 in.), and at three different deflection angles to the airfoil chord (30, 45, and 60 deg).

### Wind-Tunnel Apparatus and Test Procedure

The airfoil was tested in the Air Force Institute of Technology 5-foot wind tunnel. The wind tunnel is an open-circuit-type tunnel with a maximum air-flow speed of approximately 300 mph. The tests were normally run at approximately 75 and 95 fps. Two large wooden side panels were installed in the 5-ft-diam circular test section to provide a two-dimensional test section that was 60 in. high by 30 in. wide. Four pitot-static tubes were used to measure the local dynamic pressure near the entrance to the two-dimensional test section. Adjustments to the side walls were made to provide uniform flow in the test section. The two-dimensionality was further increased by using large circular, 0.19-in.-thick, beveled endplates on the ends of the airfoil to reduce the boundary layer that formed on the wooden side panels.

A total head wake survey rake was designed and constructed to obtain the profile drag of the airfoil. The rake

consisted of 96 total pressure tubes spaced 0.25 in. apart at the airfoil section. There were also two static pressure tubes. The rake was located 1.85 chord lengths behind the airfoil. Red-oil manometers inclined at 60 deg were connected to the rake tubes. The manometer readings were obtained from photographs of the manometer bank. Forty-eight alcohol manometers were used for indicating the airfoil upper and lower surface static pressures. The manometer readings also were obtained from photographs of the manometer bank.

Preliminary tests showed that the flow across the airfoil was essentially two-dimensional and that the blowing air was uniform along the airfoil span. The blowing air was obtained from a compressor that was separate from the wind tunnel. The blowing air flowrate was measured with an orifice meter prior to entering the airfoil.

Tests were performed on the airfoil over an angle of attack range from  $-6$  to  $16$  deg in at least 2-deg increments; however, many of the tests were limited to a  $-6$  to  $6$  deg range. Usually the runs were repeated for accuracy checks over a portion of the range. Standard wind-tunnel corrections were applied to the experimental data.<sup>10</sup> The blowing rates were varied to provide a momentum coefficient range from  $C_\mu = 0.01$  to  $C_\mu = 0.9$ , whereas the tunnel was operated at or near two different Reynolds numbers:  $7.6 \times 10^5$  and  $1.1 \times 10^6$ . Some typical circulation control jet exit velocities  $V_j$  were, for example, approximately 275 fps at  $C_\mu = 0.03$ , approximately 350 fps at  $C_\mu = 0.05$ , and approximately 450 fps at  $C_\mu = 0.09$ . The jet exit velocity was determined by assuming isentropic flow through the blowing slot in a manner similar to that used by Walters et al.<sup>3</sup> The splitter plate configurations also were varied throughout the tests.

The experimental data obtained during the tests were reduced to three section parameters: the momentum coefficient  $C_\mu$ , lift coefficient  $C_l$ , and the total drag coefficient  $C_d$ . With these parameters, lift-to-drag ratio  $L/D$  also could be obtained. The total drag coefficient used herein is similar to the total drag coefficient of Kind and Maull<sup>1</sup> and the equivalent force-based drag coefficient of Engler and Williams<sup>11</sup>; that is

$$C_d = C_{dr} - \frac{mV_0}{q_0c} + C_\mu = C_{dr} - C_\mu \frac{V_0}{V_j} + C_\mu \quad (1)$$

where

$$C_{dr} = \frac{2}{c} \int_0^h \left( \sqrt{\frac{q}{q_0}} - \frac{q}{q_0} \right) dy \quad (2)$$

and

$$C_\mu = mV_j / q_0c \quad (3)$$

The first term in Eq. (1) represents the profile drag measured by the wake rake.<sup>10,12</sup> The second term provides a correction to the drag to account for the circulation control jet.<sup>1,4,11</sup> The third term  $C_\mu$  is needed to avoid zero or negative values of  $C_{dr}$  (corrected) that occur at the higher blowing rates. The inclusion of  $C_\mu$  also accounts for some of the performance penalty incurred to provide the blowing air.<sup>1,11</sup> The integration required to compute  $C_{dr}$  was performed by numerical integration using a calculator with a digitizer.

The section parameters are presented only in terms of the geometric angle of attack  $\alpha$ . However, a relatively low aspect ratio airfoil was used in this study and the geometric angle of attack should be corrected to an effective angle of attack  $\alpha_{eff}$  due to downwash induced by the end wall vortices. This correction is discussed at length by Kind and Maull,<sup>1</sup> Engler and Williams,<sup>11</sup> and Walters et al.<sup>3</sup> These studies show that as the lift coefficient increases the induced angle of attack  $\alpha_i$  increases and the difference between  $\alpha$  and  $\alpha_{eff}$  increases. For example, for a  $C_l$  of 2,  $\alpha_{eff}$  may be several degrees less than  $\alpha$ .<sup>1,3,11</sup> This correction is discussed further in the next section when it is used to correlate experimental and theoretical pressure distributions.

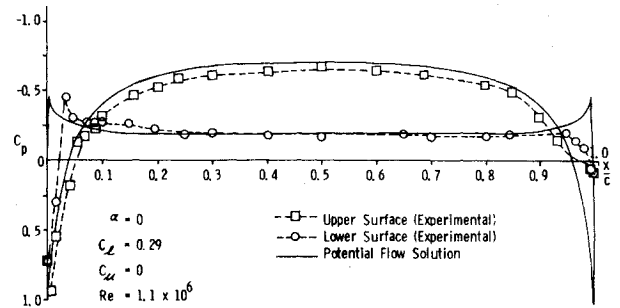


Fig. 3 Airfoil pressure distributions without splitter plate (clean) and without blowing.

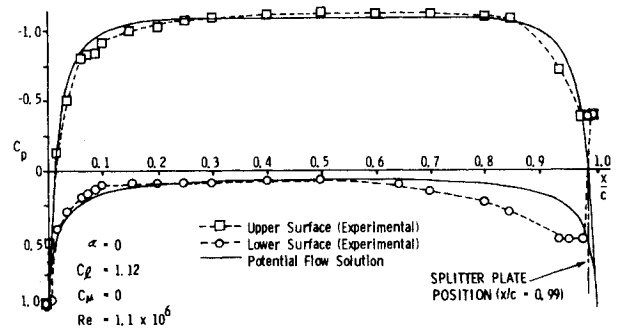


Fig. 4 Airfoil pressure distributions with splitter plate and without blowing.

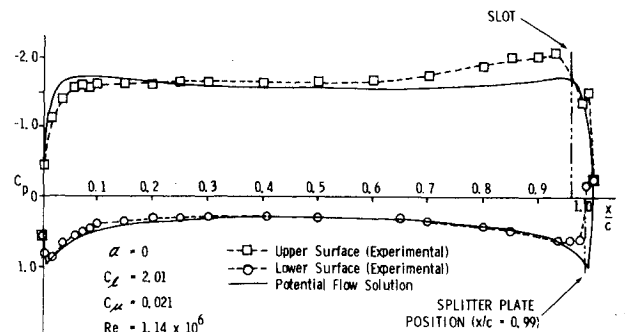


Fig. 5 Airfoil pressure distributions with splitter plate and with blowing.

## Results and Discussion

The results of the wind tunnel tests are shown in Figs. 3-12. Figures 3-5 present some airfoil experimental pressure distributions at zero geometric angle of attack for three different cases: 1) no blowing and no splitter plate (clean airfoil), 2) no blowing with a splitter plate, and 3) blowing with a splitter plate. The splitter plate used for these particular tests had a 1.5-in. chord and a deflection angle of approximately 45 deg, but was not tapered as shown in Fig. 2. Potential flow solutions also are shown in Figs. 3-5. The pressure distributions illustrate the significant increases in lift due to blowing and the use of a splitter plate.

Theodorsen's method was used to determine the theoretical potential flow pressure distributions over the airfoil for each experimentally determined lift coefficient at the same angle of attack. Although reasonably good agreement was obtained between the experimental data and the potential flow solutions, Fig. 5 tends to show an angle of attack difference between experiment and theory. These differences are most likely due to downwash. The procedure given by Ness<sup>13</sup> was used to compute a downwash correction. For a lift coefficient of 2.01 this correction was on the order of 1 deg.

Although the differences between the geometric and effective angles of attack increase as the lift coefficient in-

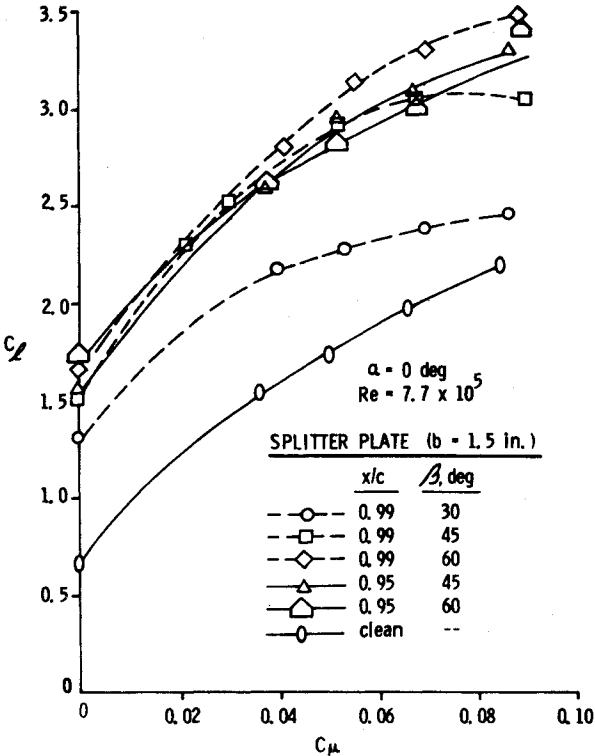


Fig. 6 Effect of blowing rate on section lift coefficient for various splitter plate configurations.

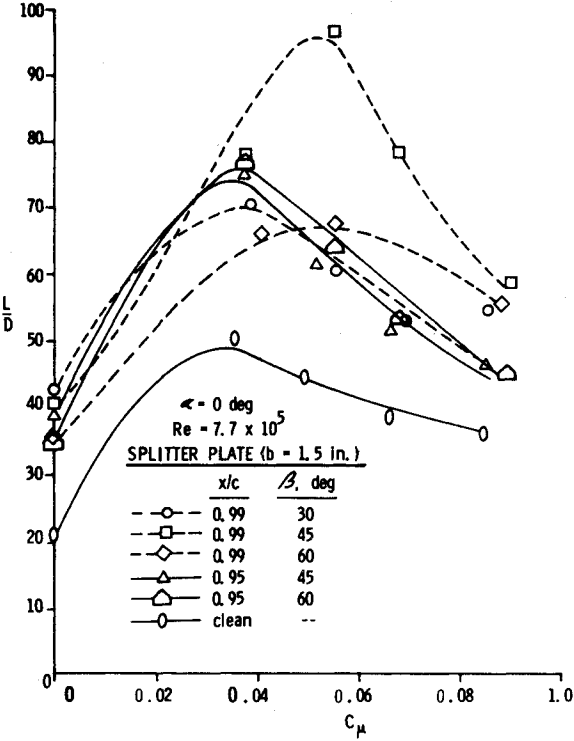


Fig. 8 Effect of blowing rate on section lift-to-drag ratio for various splitter plate configurations.

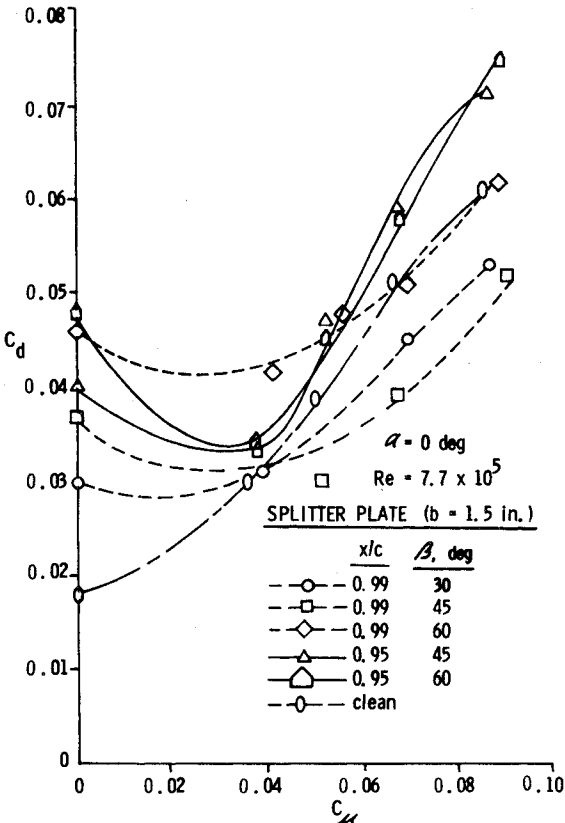


Fig. 7 Effect of blowing rate on section drag coefficient for various splitter plate configurations.

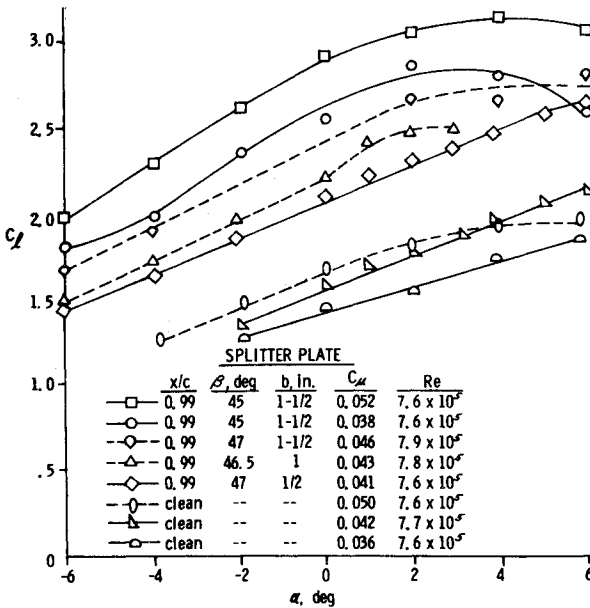


Fig. 9 Effect of splitter plate chord on lift coefficient.

creases, it was decided in this study to show the relative effectiveness of the blowing and the use of a splitter plate using geometric angles of attack only.

The effects of blowing rate and splitter plate configuration on lift and drag are shown in Figs. 6 and 7 where  $C_l$  is shown

to generally increase with increase in  $C_{\mu}$ , whereas  $C_d$  decreases first and then increases with increasing values of  $C_{\mu}$ , except for the clean configuration where no splitter plate was used. The results also depend on the splitter plate configuration. The section  $L/D$  for each configuration is shown in Fig. 8 to generally increase with blowing, reach a maximum, and then decrease with further increases in blowing rates. The dependence of the results on splitter plate configuration also is apparent. It can be seen in Fig. 8 that the highest  $L/D$  occurred with the aft, 45-deg, 1.5-in. splitter plate configuration. For this configuration in the range of  $C_{\mu} = 0.05$ , the  $L/D$  is approximately double that for the clean configuration, whereas for the other splitter plate configurations, the increases over the clean configuration are

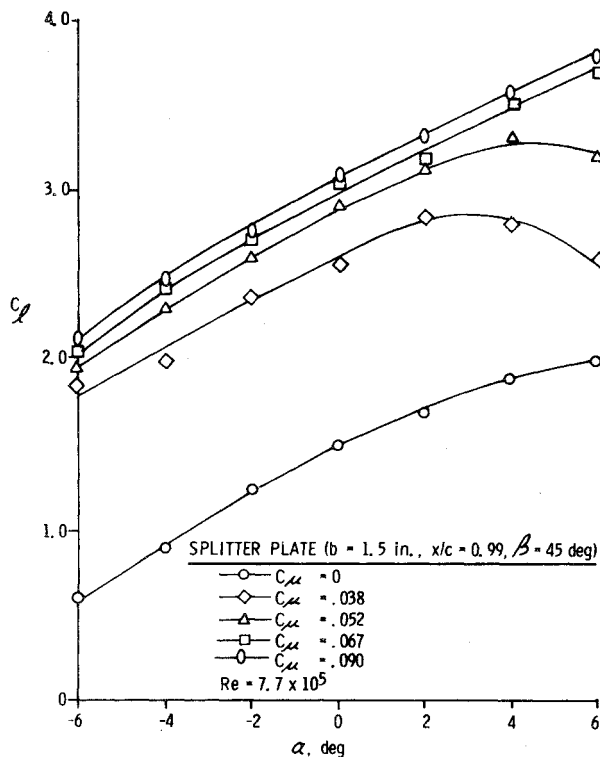


Fig. 10 Variation of lift coefficient with angle of attack at various blowing rates.

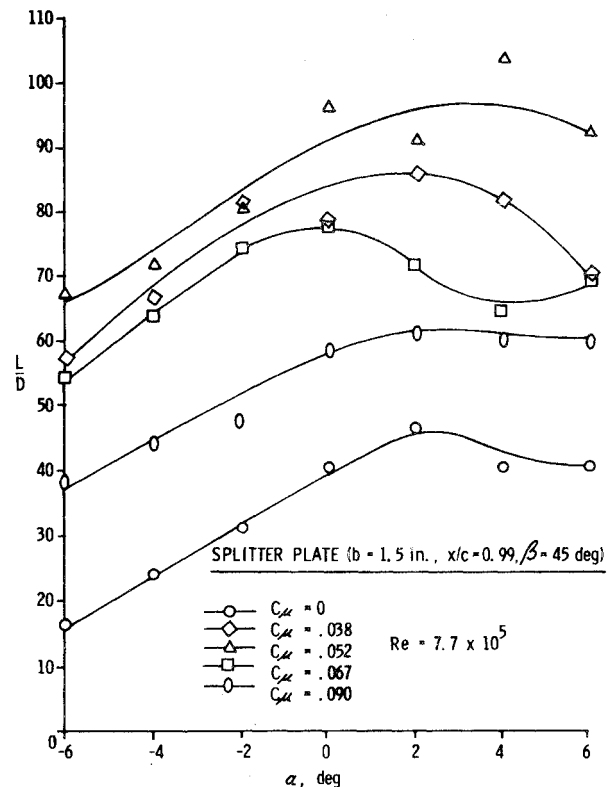


Fig. 12 Variation of lift-to-drag ratio with angle of attack at various blowing rates.

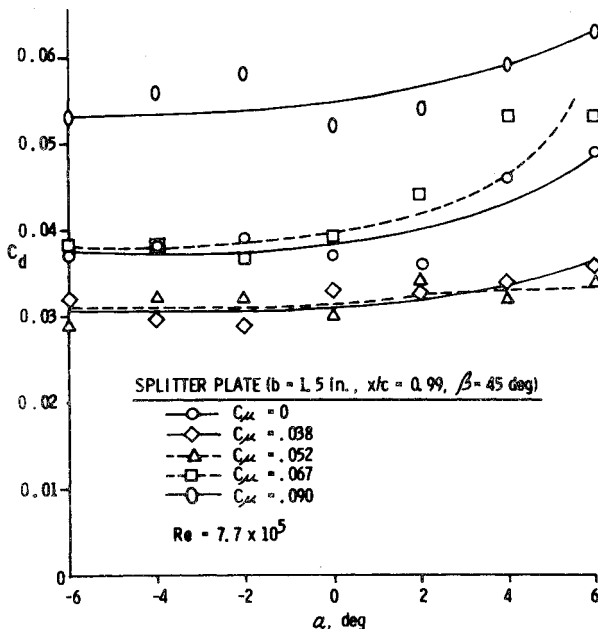


Fig. 11 Variation of drag coefficient with angle of attack at various blowing rates.

only on the order of 50%. For these results (Figs. 6-8), the 1.5-in. splitter plate was used and the airfoil was at zero degrees angle of attack.

The effect of splitter plate chord on  $C_l$  for the aft-45 deg splitter plate configuration is shown in Fig. 9. The results indicate that the lift coefficient increases with increases in splitter plate chord. Thus, the 1.5-in. chord splitter plate was used in the majority of the test.

The effects of angle of attack on  $C_l$ ,  $C_d$ , and  $L/D$  are shown in Figs. 10, 11, and 12, respectively, for the aft, 45-deg, 1.5-in. splitter plate configuration. The results (Fig. 10) indicate that  $C_l$  increases with increases in  $C_\mu$  over the entire

range of negative angles of attack tested. In some cases, separation occurred at positive angles of attack. Separation at any angle of attack depended on blowing rate, Reynolds number, and splitter plate configuration. Generally, separation and the effects on  $C_l$  was more abrupt when the splitter plate was not used. The effects of angle of attack on  $C_d$  and  $L/D$  are shown in Figs. 11 and 12, respectively. The trends noted previously at zero angle of attack (Figs. 6-8) are shown to be approximately the same over the angles of attack shown.

### Conclusions

- 1) The lift of the elliptical airfoil is increased significantly by blowing air along the upper surface near the trailing edge, even at negative angles of attack.
- 2) The addition of a splitter plate increases the lift-to-drag ratio on a circulation-controlled airfoil.
- 3) The lift coefficient increases as the chord of the splitter plate is increased.
- 4) The lift-to-drag ratio was maximum for momentum coefficients generally in the range of 0.02 to 0.06.
- 5) Of the configurations tested, the highest lift-to-drag ratio was obtained with the aft, 45-deg, 1.5-in. splitter plate.

### Acknowledgment

The views expressed herein are those of the authors and do not necessarily reflect those of the U. S. Air Force nor the Department of Defense.

### References

- 1 Kind, R. J. and Maull, D. J., "An Experimental Investigation of a Low Speed Circulation-Controlled Aerofoil," *The Aeronautical Quarterly*, Vol. 19, May 1968, pp. 170-182.
- 2 Englar, R. J., "Two-Dimensional Subsonic Wind Tunnel Tests of Two 15-Percent Thick Circulation Control Airfoils," Naval Ship Research and Development Center, Bethesda, Md., AD900210, NSRDC Technical Note AL-211, Aug. 1971.
- 3 Walters, R. E., Myer, D. P., and Holt, D. J., "Circulation Control by Steady and Pulsed Blowing for a Cambered Elliptical

Airfoil," West Virginia University, Morgantown, West Va., AD751045, Aerospace Engineering TR-32, July 1972.

<sup>4</sup>Williams, R. M. and Howe, H. J., "Two Dimensional Subsonic Wind Tunnel Tests on a 20 Percent Thick, 5 Percent Cambered Circulation Control Airfoil," Naval Ship Research and Development Center, Bethesda, Md., AD877764, NSRDC Technical Note AL-176, Aug. 1970.

<sup>5</sup>Bauer, A. B., "A New Family of Airfoils Based on the Jet-Flap Principle," Douglas Aircraft Company, Long Beach, Calif., Report No. MDC J5713, Sept. 1972.

<sup>6</sup>McCormick, B. W. Jr., *Aerodynamics of V/STOL Flight*, Academic Press, New York, 1967.

<sup>7</sup>Smith, A. M. O. and Thelander, J. A., "The Power Profile A New Type of Airfoil," Douglas Aircraft Company, Long Beach, Calif., Report No. MDC J6263, Jan. 1974.

<sup>8</sup>Loth, J. L., Fanucci, J. B., and Roberts, S. C., "Flight Performance of a Circulation Controlled STOL Aircraft," *Journal of Aircraft*, Vol. 13, March 1976, pp. 169-173.

<sup>9</sup>Engler, R. J., "Circulation Control for High Lift and Drag Generation on STOL Aircraft," *Journal of Aircraft*, Vol. 12, May 1975, pp. 457-463.

<sup>10</sup>Pope, A., *Wind-Tunnel Testing*, 2nd ed., Wiley, New York, 1954.

<sup>11</sup>Engler, R. J. and Williams, R. M., "Test Techniques for High-Lift, Two-Dimensional Airfoils with Boundary Layer and Circulation Control for Application to Rotary Wing Aircraft," Naval Ship Research and Development Center, Bethesda, Md., NSRDC Report 4645, July 1975.

<sup>12</sup>Schlichting, H., *Boundary-Layer Theory*, 6th ed., McGraw-Hill Book Company, New York, 1968.

<sup>13</sup>Ness, N., "Downwash Correction for a Two-Dimensional Finite Wing," *Journal of Aircraft*, Vol. 8, Sept. 1971, pp. 745-746.

## *From the AIAA Progress in Astronautics and Aeronautics Series*

### **AEROACOUSTICS:**

**JET NOISE; COMBUSTION AND CORE ENGINE NOISE—v. 43**

**FAN NOISE AND CONTROL; DUCT ACOUSTICS; ROTOR NOISE—v. 44**

**STOL NOISE; AIRFRAME AND AIRFOIL NOISE—v. 45**

**ACOUSTIC WAVE PROPAGATION; AIRCRAFT NOISE PREDICTION;  
AEROACOUSTIC INSTRUMENTATION—v. 46**

*Edited by Ira R. Schwartz, NASA Ames Research Center, Henry T. Nagamatsu, General Electric Research and Development Center, and Warren C. Strahle, Georgia Institute of Technology*

The demands placed upon today's air transportation systems, in the United States and around the world, have dictated the construction and use of larger and faster aircraft. At the same time, the population density around airports has been steadily increasing, causing a rising protest against the noise levels generated by the high-frequency traffic at the major centers. The modern field of aeroacoustics research is the direct result of public concern about airport noise.

Today there is need for organized information at the research and development level to make it possible for today's scientists and engineers to cope with today's environmental demands. It is to fulfill both these functions that the present set of books on aeroacoustics has been published.

The technical papers in this four-book set are an outgrowth of the Second International Symposium on Aeroacoustics held in 1975 and later updated and revised and organized into the four volumes listed above. Each volume was planned as a unit, so that potential users would be able to find within a single volume the papers pertaining to their special interest.

v. 43—648 pp., 6 x 9, illus. \$19.00 Mem. \$40.00 List  
v. 44—670 pp., 6 x 9, illus. \$19.00 Mem. \$40.00 List  
v. 45—480 pp., 6 x 9, illus. \$18.00 Mem. \$33.00 List  
v. 46—342 pp., 6 x 9, illus. \$16.00 Mem. \$28.00 List

*For Aeroacoustics volumes purchased as a four-volume set: \$65.00 Mem. \$125.00 List*

TO ORDER WRITE: Publications Dept., AIAA, 1290 Avenue of the Americas, New York, N. Y. 10019